Breast Cancer Research and Treatment (2019) 177:651–657
https://doi.org/10.1007/s10549-019-05339-0

CLINICAL TRIAL

The relationship between ring-type dedicated breast PET and immune microenvironment in early breast cancer

Shinsuke Sasada[1] · Noriyuki Shiroma[2] · Noriko Goda[1] · Keiko Kajitani[1] · Akiko Emi[1] · Norio Masumoto[1] · Takayuki Kadoya[1] · Koji Arihiro[2] · Morihito Okada[1]

Received: 12 July 2018 / Accepted: 27 June 2019 / Published online: 2 July 2019
© Springer Science+Business Media, LLC, part of Springer Nature 2019

Abstract

Purpose ^{18}F-fluorodeoxyglucose (FDG) uptake on positron emission tomography (PET) is related to the biological parameters and prognosis of breast cancer. However, whether whole-body PET (WBPET) and dedicated breast PET (DbPET) can reflect the tumor microenvironment is unclear. This study investigated the relationship between stromal tumor-infiltrating lymphocytes (TILs) and maximum standardized uptake value (SUVmax) in WBPET and DbPET.

Methods A total of 125 invasive breast cancers underwent WBPET and ring-type DbPET and resected specimens were pathologically assessed. The impact of SUVmax on the tumor biological parameters and TILs was retrospectively evaluated. SUVmax was classified as high and low relative to the median values (WBPET-SUVmax: 2.2 and DbPET-SUVmax: 6.0).

Results SUVmax correlated with tumor size, nuclear grade, Ki-67 labeling index, and TILs in both WBPET and DbPET (all $p < 0.001$). In multiple linear regression analysis, tumor size, Ki-67 labeling index, and TILs predicted SUVmax in WBPET and DbPET. The cutoff values of tumor size, Ki-67 labeling index, and TILs predicting high SUVmax were 20 mm, 20%, and 20%, respectively. In multivariate analysis, the predictive factors for high SUVmax were tumor size and Ki-67 labeling index for WBPET and tumor size and TILs for DbPET. High SUVmax in DbPET was related to high numbers of TILs after propensity score matching analysis; however, WBPET was not ($p = 0.007$ and $p = 0.624$, respectively).

Conclusions Both SUVmax values in WBPET and DbPET predicted TIL concentration of the primary breast cancer. In DbPET, SUVmax represented the immune microenvironment after adjusting for tumor biological factors.

Keywords Breast cancer · Dedicated breast PET · FDG · SUV · Tumor-infiltrating lymphocyte · Tumor microenvironment

Abbreviations

CTLA-4	Cytotoxic T-lymphocyte-associated protein 4
DbPET	Dedicated breast positron emission tomography
ER	Estrogen receptor
FDG	^{18}F-fluorodeoxyglucose
FOV	Field of view
FOXP3	Forkhead box P3
HER2	Human epidermal growth factor receptor 2
IC-NST	Invasive carcinoma of no special type
OR	Odds ratio
PD-1	Programmed cell death-1
PET	Positron emission tomography
SUVmax	Maximum standardized uptake value
TIL	Tumor-infiltrating lymphocytes
TNBC	Triple-negative breast cancer
WBPET	Whole-body positron emission tomography

Introduction

Breast cancer consists of tumor cells and the tumor microenvironment. Tumor-infiltrating lymphocytes (TILs) activated in the tumor microenvironment express cytotoxic T-lymphocyte-associated protein 4 (CTLA-4) and programmed cell death-1 (PD-1) and play an important role in the immune system [1]. TIL expression is high in human epidermal growth factor receptor 2 (HER2)-positive and triple-negative breast cancer (TNBC) [2]. High TIL is a

✉ Shinsuke Sasada
shsasada@hiroshima-u.ac.jp

[1] Department of Surgical Oncology, Research Institute for Radiation Biology and Medicine, Hiroshima University, 1-2-3 Kasumi, Minami-Ku, Hiroshima, Hiroshima 734-8551, Japan

[2] Department of Anatomical Pathology, Hiroshima University Hospital, Hiroshima, Japan

favorable prognostic factor, especially in early HER2-positive breast cancer and TNBC [3, 4].

^{18}F-fluorodeoxyglucose-positron emission tomography (FDG-PET) is a molecular approach that uses glucose metabolism for cancer imaging. FDG is taken up not only in tumor cells but also in inflammatory cells by the Warburg effect [5]. Correlations between whole-body PET (WBPET) and immune markers have been reported only in gastric and non-small cell lung cancers [6, 7]. The maximum standardized uptake value (SUVmax) was significantly correlated with levels of forkhead box P3 (FOXP3), a biomarker of regulatory T cell, in gastric cancer ($r = 0.431$, $p < 0.001$) [6], and CD8-positive TILs ($r = 0.308$, $p = 0.027$) and PD-1 ($r = 0.325$, $p = 0.017$) in non-small cell lung cancer [7].

Dedicated breast PET (DbPET) was developed for high-resolution molecular breast imaging and detection of subcentimeter breast tumors. In addition, DbPET can be used to visualize intratumoral heterogeneity such as central necrosis [8]. Unlike other scanner types, the three-dimensional imaging of ring-type DbPET can be used to calculate the SUV value [9].

Therefore, we hypothesized that ring-type DbPET could be used to visualize not only the tumor cells but also the tumor microenvironment more clearly than WBPET. We investigated whether the SUVmax value by DbPET reflected the TILs in the tumor immune tumor microenvironment compared to that with WBPET. To our knowledge, this is the first report to consider the relationship between DbPET and TILs in breast cancer.

Patients and methods

Patients

Among consecutive 277 patients with breast cancers who underwent complete resection between January and December 2016 at Hiroshima University Hospital, 199 patients (211 tumors) received WBPET and ring-type DbPET. Of them, tumors that received neoadjuvant chemotherapy, non-invasive carcinoma, and unevaluable stromal TILs were excluded and a total of 125 breast cancers were retrospectively assessed (Fig. 1). The Institutional Review Board of Hiroshima University Hospital approved this study. All procedures performed in studies involving human participants were in accordance with the ethical standards of the institutional research committee and with the 1964 Helsinki Declaration and its later amendments or comparable ethical standards. For this type of study, formal consent is not required.

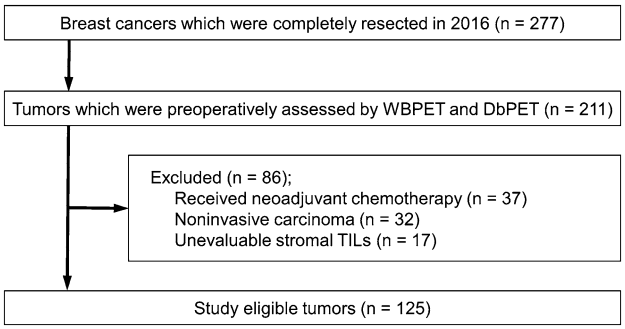

Fig. 1 Study profile

WBPET and DbPET examinations

All DbPET examinations were performed at the same time as WBPET. The patients fasted for at least 4 h before the FDG injection (3–3.7 MBq/kg). WBPET scanning was performed 1 h after the FDG administration using a Discovery ST16 PET/computed tomography (CT) scanner (GE Healthcare, Little Chalfont, UK; BGO/6.25 × 6.25 × 30 mm). Low-dose non-enhanced CT images (3- to 4-mm slice thickness) for attenuation correction and localization of lesions identified using PET were obtained from the head to the pelvic floor of each patient according to a standard protocol. Immediately after CT, the identical axial field of view (FOV) (154 mm) was scanned using PET for 2–3 min per table position depending on the patient condition and the scanner performance. The acquired data were reconstructed as 128 × 128 matrix images (pixel size, 4.7 × 3.25 mm) using Fourier rebinning and ordered-subset expectation maximization algorithms. Both PET and CT studies were performed with the patient under normal tidal breathing.

Immediately after WBPET, DbPET was performed using an Elmammo scanner (Shimadzu, Kyoto, Japan; LGSO/1.44 × 1.44 × 18 mm) while patients were in the prone position. The FOV was 185 × 156.5 mm, the scan time was 7 min per bed position, and the acquired data were reconstructed as 236 × 236 matrix images (pixel size, 0.78 × 0.78 mm) using a three-dimensional dynamic row-action maximum likelihood algorithm.

PET image evaluation and quantification of the SUVmax were performed using an Xeleris workstation version 1.1452 (GE Healthcare, Little Chalfont, UK). Regions of interest were first delineated within the primary tumor on attenuation-corrected FDG-PET images and within the ipsilateral normal breast tissue for the background uptake and SUVmax was then measured. The attenuation correction of DbPET was carried out as a homogeneous soft tissue of breast tissue composed of mammary glands and

fat. All PET images were read by two professionals: a radiologist and a breast cancer specialist.

Pathological diagnosis

The breast tumor samples were collected via surgery. The histopathological characteristics, such as histology, nuclear grade, hormonal receptors and HER2 status, Ki-67 labeling index, and stromal TILs were evaluated. Hormonal receptors and HER2 were assessed by American Society of Clinical Oncology/College of American Pathologists Guidelines [10, 11]. The evaluation of stromal TILs was based on recommendations from the International TILs Working Group 2014 [12].

Statistics

The summarized data are presented as numbers and percentages unless otherwise stated. Frequencies were compared using Fisher's exact test for categorical variables. Meanwhile, continuous variables were compared using Mann–Whitney *U* test or one-way analysis of variance. Correlation analyses were performed using Spearman's rank correlation coefficients. Multiple linear regression analysis using a stepwise method based on *P* value and logistic regression analysis was used to predict the SUVmax. The SUVmax values in WBPET and DbPET were classified into two groups based on the median value. Receiver operating characteristic curves were drawn to determine the cutoff values of parameters predicting high SUVmax. A 1:1 paired matching according to propensity scores, including tumor size, nuclear grade, and Ki-67 labeling index, was applied separately on low- and high-TIL tumors. $p < 0.05$ was considered statistically significant. All statistical analyses were performed using EZR (Saitama Medical Center, Jichi Medical University, Saitama, Japan), which is a graphical user interface for R (The R Foundation for Statistical Computing, Vienna, Austria) [13].

Results

The characteristics of the 122 patients (125 tumors) are summarized in Table 1. Most tumors were invasive carcinoma of no special type, estrogen receptor (ER)-positive, and HER2-negative. The SUVmax in DbPET was about three times that in WBPET (median: 6.0 and 2.2, respectively). The SUVmax values in WBPET and DbPET were significantly related to tumor size ($r = 0.630$ and 0.528, respectively), Ki-67 labeling index ($r = 0.507$ and 0.456, respectively), TILs ($r = 0.313$ and 0.376, respectively), and nuclear grade (Fig. 2). Multiple linear regression analysis revealed that tumor size, Ki-67 labeling index, and TIL concentration were significant predicting factors of SUVmax in both WBPET and DbPET ($R^2 = 0.447$ and 0.421, respectively) (Table 2). Histology, nuclear grade, ER, and HER2 were not related with the SUVmax in WBPET and DbPET.

Table 1 Patient characteristics

	Number (%)
Age (years), median (range)	57 (30–86)
T status	
1	79 (63.2)
2	44 (35.2)
3	2 (1.6)
N status	
0	93 (74.4)
1	29 (23.2)
2	2 (1.6)
3	1 (0.8)
Histology	
Microinvasive carcinoma	4 (3.2)
Invasive carcinoma of no special type	103 (82.4)
Invasive lobular carcinoma	5 (4.0)
Others	13 (10.4)
Nuclear grade	
1	21 (16.8)
2	53 (42.4)
3	51 (40.8)
Ki-67 labeling index (%), median (IQR)	28 (14–42)
ER positive	119 (95.2)
PgR positve	114 (91.2)
HER2 positive	9 (7.2)
SUVmax, median (IQR)	
WBPET	2.2 (1.3–3.5)
DbPET	6.0 (3.5–10.0)
Tumor infiltrating lymphocytes (%), median (IQR)	5 (1–20)

DbPET dedicated breast positron emission tomography, *ER*,estrogen receptor, *HER2* human epidermal growth factor receptor 2, *IQR* interquartile range, *PgR* progesterone receptor, *SUVmax* maximum standardized uptake value, *WBPET* whole-body positron emission tomography

The cutoffs of tumor size, Ki-67 labeling index, and TIL concentration predicting high SUVmax in WBPET and DbPET were 20 mm, 20%, and 20%, respectively. In multivariate logistic regression analyses, the factors predicting high SUVmax in WBPET were larger tumor size and high Ki-67 labeling index (odds ratio [OR] 13.0, $p < 0.001$ and OR 3.68, $p = 0.020$, respectively). Meanwhile, the predictors for high SUVmax in DbPET were tumor size and high TILs (OR 4.81, $p < 0.001$ and OR 6.98, $p < 0.001$, respectively) (Table 3). Figure 3 shows representative images of WBPET and DbPET according to TIL rates in breast cancers with the same histology, tumor size, nuclear grade, Ki-67 labeling index, and ER and HER2 status.

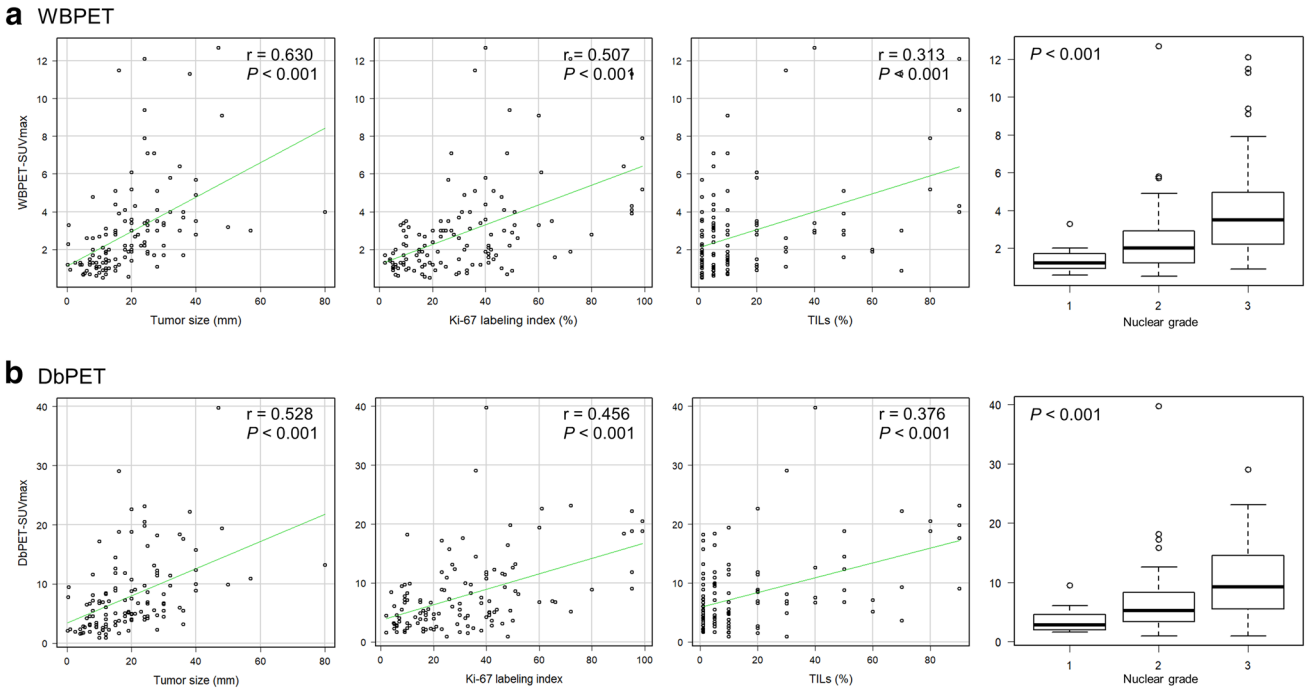

Fig. 2 Correlations between SUVmax on WBPET (**a**) and DbPET (**b**), and tumor factors. *DbPET* dedicated breast positron emission tomography, *TIL* tumor-infiltrating lymphocyte, *WBPET* whole-body positron emission tomography

Table 2 Stepwise multiple linear regression analysis for factors influencing SUVmax in WBPET and DbPET

Factors	Regression coefficient (95% CI)	Standard error	*t*	*p*
<WBPET>				
Intercept	0.13 (−0.54 to 0.8)	0.34	0.39	0.690
Tumor size	0.07 (0.05–0.1)	0.01	5.52	< 0.001
Ki-67 labeling index	0.03 (0.01–0.04)	0.01	3.33	0.001
TILs	0.03 (0.01–0.04)	0.01	3.42	< 0.001
<DbPET>				
Intercept	0.90 (−0.96 to 2.75)	0.94	0.96	0.340
Tumor size	0.19 (0.12–0.26)	0.04	5.15	< 0.001
Ki-67 labeling index	0.06 (0.02–0.11)	0.02	2.74	0.007
TILs	0.08 (0.04–0.13)	0.02	3.65	< 0.001

CI confidence interval, *DbPET* dedicated breast positron emission tomography, *SUVmax* maximum standardized uptake value, *TIL* tumor infiltrating lymphocyte, *WBPET* whole-body positron emission tomography

The propensity score matching analysis using tumor size, nuclear grade, and Ki-67 labeling index is summarized in Table 4. The tumor biological factors were balanced between low- and high-TIL tumors. Although high-TIL tumors were unrelated to high SUVmax in WBPET ($p=0.624$), the correlation between high-TIL tumors and high SUVmax in DbPET was significant ($p=0.007$).

Discussion

This study demonstrated the relationship between ring-type DbPET and the immune microenvironment in early breast cancer. The SUVmax in both WBPET and DbPET predicted TILs rates of breast tumors as well as tumor

Table 3 Logistic regression analysis for predicting high SUVmax on WBPET and DbPET

Factors	Univariate analysis		Multivariate analysis	
	OR (95% CI)	*p*	OR (95% CI)	*p*
<WBPET>				
Histology_IC-NST	6.71 (1.87–24.1)	0.003	1.35 (0.37–4.97)	0.655
T2–3	6.18 (2.76–13.8)	< 0.001	13.00 (4.41–38.30)	< 0.001
Nuclear grade 3	6.48 (2.94–14.3)	< 0.001	2.70 (0.92–7.91)	0.071
ER positive	0.39 (0.07–2.20)	0.285	0.32 (0.02–4.76)	0.404
HER2 positive	1.62 (0.42–6.37)	0.486	0.31 (0.05–1.95)	0.211
Ki-67 labeling index ≥ 20%	3.03 (1.39–6.61)	0.005	3.68 (1.23–11.10)	0.020
TILs ≥ 20%	1.99 (0.91–4.33)	0.084	2.29 (0.75–6.93)	0.144
<DbPET>				
Histology_IC-NST	3.18 (1.15–8.77)	0.003	1.68 (0.51–5.50)	0.393
T2–3	4.38 (1.99–9.63)	< 0.001	4.81 (1.91–12.20)	< 0.001
Nuclear grade 3	4.43 (2.05–9.56)	< 0.001	1.82 (0.67–4.90)	0.238
ER positive	0.98 (0.69–1.40)	0.929	0.70 (0.08–6.60)	0.758
HER2 positive	0.97 (0.68–1.38)	0.857	0.53 (0.10–2.73)	0.450
Ki-67 labeling index ≥ 20%	3.54 (1.63–7.67)	0.001	1.39 (0.52–3.71)	0.513
TILs ≥ 20%	7.50 (2.96–19.0)	< 0.001	6.98 (2.37–20.50)	< 0.001

CI confidence interval, *DbPET* dedicated breast positron emission tomography, *ER* estrogen receptor, *HER2* human epidermal growth factor receptor 2, *IC-NST* invasive carcinoma of no special type, *OR* odds ratio, *SUVmax* maximum standardized uptake value, *TIL* tumor infiltrating lymphocyte, *WBPET* whole-body positron emission tomography

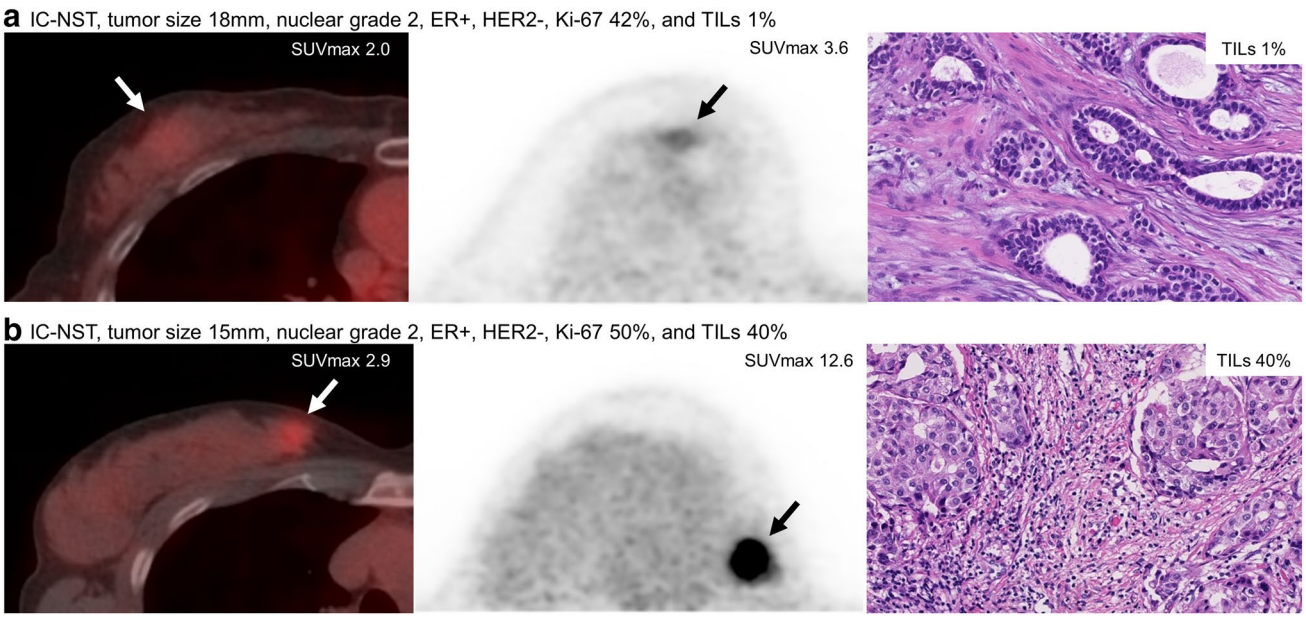

Fig. 3 Representative images of WBPET and DbPET according to TILs rate adjusted for tumor biological features. Low TILs tumor (**a**), high TILs tumor (**b**), WBPET image (left), DbPET image (center), and TILs rate according to histological findings (right). *DbPET* dedicated breast positron emission tomography, *ER* estrogen receptor, *HER2* human epidermal growth factor receptor 2, *IC-NST* invasive carcinoma of no special type, *TIL* tumor-infiltrating lymphocyte, *WBPET* whole-body positron emission tomography

Table 4 Characteristics of propensity score matched patients according to TIL rate

	Low TILs	High TILs	*p*
Age (years), median (range)	58 (36–77)	48 (30–80)	0.230
T status			0.683
1	20 (54.1)	23 (62.2)	
2	17 (45.9)	14 (37.8)	
3	0 (0)	0 (0)	
N status			0.637
0	22 (70.3)	27 (73.0)	
1	10 (27.0)	9 (24.3)	
2	0 (0)	1 (2.7)	
3	1 (2.7)	0 (0)	
Histology			1
Microinvasive carcinoma	1 (2.7)	0 (0)	
Invasive carcinoma of no special type	34 (91.9)	35 (94.6)	
Invasive lobular carcinoma	0 (0)	1 (2.7)	
Others	2 (5.4)	1 (2.7)	
Nuclear grade			0.850
1	2 (5.4)	1 (2.7)	
2	12 (32.4)	11 (29.7)	
3	23 (62.2)	25 (67.6)	
Ki-67 labeling index (%), median (IQR)	40 (29–46)	40 (30–65)	0.111
ER positive	35 (94.6)	34 (91.9)	1
PgR positve	31 (83.8)	33 (89.2)	0.736
HER2 positive	4 (10.8)	4 (10.8)	1
WBPET-SUVmax			0.624
Low	14 (37.8)	11 (29.7)	
High	23 (62.2)	26 (70.3)	
DbPET-SUVmax			0.007
Low	19 (51.4)	7 (18.9)	
High	18 (48.6)	30 (81.1)	

DbPET dedicated breast positron emission tomography, *ER* estrogen receptor, *HER2* human epidermal growth factor receptor 2, *IQR* interquartile range, *PgR* progesterone receptor, *SUVmax* maximum standardized uptake value, *TIL* tumor infiltrating lymphocyte, *WBPET* whole-body positron emission tomography

size and Ki-67 labeling index, and the SUVmax in DbPET reflected TILs after adjusting for tumor biological factors.

FDG-PET can be used to visualize glucose metabolism in tumors and the SUVmax in WBPET can predict malignant behavior and prognosis in early breast cancer [14–16]. In addition, WBPET after two cycles or completion of neoadjuvant chemotherapy may be useful to predict pathological complete response [17, 18]. However, WBPET before chemotherapy could not predict pathological response [17]. Recently, we have reported ring-type DbPET to be more accurate than WBPET in detecting residual primary tumors after neoadjuvant chemotherapy [19]. DbPET is a high-resolution molecular breast imaging device; the sensitivity of opposite-type DbPET was 92–95%, higher than that of WBPET [20]. The sensitivity of ring-type DbPET scanners, such as Mammi-PET and Elmammo, was 82–100% [21–23]. As a by-product of high-resolution images, ring-type DbPET can be used to visualize intratumoral heterogeneity, such as ring-like or heterogeneous uptakes, caused by central necrosis and fibrosis [8].

TILs are key players in the tumor immune microenvironment and are abundant in HER2-positive and TNBC [2]. Increased TIL concentration is one of the predictors of pathological response to neoadjuvant chemotherapy regardless of molecular subtype [3]. Although the TIL rate is also a prognostic factor in HER2-positive and TNBC, different results have been reported for luminal-type breast cancer [3, 4]. Although the prognostic role of TILs is not consistent across subtypes, the TIL rate predicts the treatment effect. In addition, TILs expressing CTLA-4 and PD-1 are targets of immune checkpoint inhibitors. Therefore, imaging systems predicting TILs are clinically useful.

Previously, the correlations of SUVmax in WBPET and TIL-related factors have been reported only in gastric and non-small cell lung cancers, with low correlation coefficients [6, 7]. TILs activated in the tumor accumulate FDG by the Warburg effect, as do inflammatory cells [5]. However, these studies did not adjust for tumor factors that affect SUV. The strengths of our study include the use of ring-type DbPET, a novel modality for breast imaging, and adjusting for tumor factors by propensity score matching.

This study has some limitations. First, the majority of breast cancer tumors were luminal type because we excluded patients who received neoadjuvant chemotherapy. In this study, we evaluated whole tumors using resected specimens. Second, the TIL cutoff value might be specific to the present study. Different cutoffs might be required for HER2-positive and TNBC, in which TILs have more significant roles. Future studies are needed to investigate the relationship between DbPET and TIL rates in biopsy specimens as well as the response to neoadjuvant chemotherapy. Third, the subpopulations of TILs, such as regulatory T cells and cytotoxic T lymphocytes, are unknown. Immunohistochemical assessment of TILs is required.

Conclusion

SUVmax values in both WBPET and ring-type DbPET predicted the proportion of TILs of the primary breast cancer. High TILs breast cancer was significantly related to high SUVmax in DbPET after adjusting for tumor biological factors.

Acknowledgements We thank Kazushi Marukawa and Masatsugu Tsujimura of Chuden Hospital for providing PET examination data.

Compliance with ethical standards

Conflict of interest The authors declare that they have no conflict of interest.

References

1. Nishikawa H, Sakaguchi S (2014) Regulatory T cells in cancer immunotherapy. Curr Opin Immunol 27:1–7. https://doi.org/10.1016/j.coi.2013.12.005
2. Stanton SE, Adams S, Disis ML (2016) Variation in the incidence and magnitude of tumor-infiltrating lymphocytes in breast cancer subtypes: a systematic review. JAMA Oncol 2(10):1354–1360. https://doi.org/10.1001/jamaoncol.2016.1061
3. Denkert C, von Minckwitz G, Darb-Esfahani S, Lederer B, Heppner BI, Weber KE, Budczies J et al (2018) Tumour-infiltrating lymphocytes and prognosis in different subtypes of breast cancer: a pooled analysis of 3771 patients treated with neoadjuvant therapy. Lancet Oncol 19(1):40–50. https://doi.org/10.1016/s1470-2045(17)30904-x
4. Dieci MV, Mathieu MC, Guarneri V, Conte P, Delaloge S, Andre F, Goubar A (2015) Prognostic and predictive value of tumor-infiltrating lymphocytes in two phase III randomized adjuvant breast cancer trials. Ann Oncol 26(8):1698–1704. https://doi.org/10.1093/annonc/mdv239
5. Palsson-McDermott EM, O'Neill LA (2013) The Warburg effect then and now: from cancer to inflammatory diseases. BioEssays 35(11):965–973. https://doi.org/10.1002/bies.201300084
6. Lee S, Choi S, Kim SY, Yun MJ, Kim HI (2017) Potential utility of FDG PET-CT as a non-invasive tool for monitoring local immune responses. J Gastric Cancer 17(4):384–393. https://doi.org/10.5230/jgc.2017.17.e43
7. Lopci E, Toschi L, Grizzi F, Rahal D, Olivari L, Castino GF, Marchetti S et al (2016) Correlation of metabolic information on FDG-PET with tissue expression of immune markers in patients with non-small cell lung cancer (NSCLC) who are candidates for upfront surgery. Eur J Nucl Med Mol Imaging 43(11):1954–1961. https://doi.org/10.1007/s00259-016-3425-2
8. Masumoto N, Kadoya T, Sasada S, Emi A, Arihiro K, Okada M (2018) Intratumoral heterogeneity on dedicated breast positron emission tomography predicts malignancy grade of breast cancer. Breast Cancer Res Treat. https://doi.org/10.1007/s10549-018-4791-1
9. MacDonald L, Edwards J, Lewellen T, Haseley D, Rogers J, Kinahan P (2009) Clinical imaging characteristics of the positron emission mammography camera: PEM Flex Solo II. J Nucl Med 50(10):1666–1675. https://doi.org/10.2967/jnumed.109.064345
10. Hammond ME, Hayes DF, Dowsett M, Allred DC, Hagerty KL, Badve S, Fitzgibbons PL et al (2010) American Society of Clinical Oncology/College Of American Pathologists guideline recommendations for immunohistochemical testing of estrogen and progesterone receptors in breast cancer. J Clin Oncol 28(16):2784–2795. https://doi.org/10.1200/jco.2009.25.6529
11. Wolff AC, Hammond ME, Hicks DG, Dowsett M, McShane LM, Allison KH, Allred DC et al (2013) Recommendations for human epidermal growth factor receptor 2 testing in breast cancer: American Society of Clinical Oncology/College of American Pathologists clinical practice guideline update. J Clin Oncol 31(31):3997–4013. https://doi.org/10.1200/jco.2013.50.9984
12. Salgado R, Denkert C, Demaria S, Sirtaine N, Klauschen F, Pruneri G, Wienert S et al (2015) The evaluation of tumor-infiltrating lymphocytes (TILs) in breast cancer: recommendations by an International TILs Working Group 2014. Ann Oncol 26(2):259–271. https://doi.org/10.1093/annonc/mdu450
13. Kanda Y (2013) Investigation of the freely available easy-to-use software 'EZR' for medical statistics. Bone Marrow Transplant 48(3):452–458. https://doi.org/10.1038/bmt.2012.244
14. Ohara M, Shigematsu H, Tsutani Y, Emi A, Masumoto N, Ozaki S, Kadoya T et al (2013) Role of FDG-PET/CT in evaluating surgical outcomes of operable breast cancer–usefulness for malignant grade of triple-negative breast cancer. Breast (Edinburgh, Scotland) 22(5):958–963. https://doi.org/10.1016/j.breast.2013.05.003
15. Kadoya T, Aogi K, Kiyoto S, Masumoto N, Sugawara Y, Okada M (2013) Role of maximum standardized uptake value in fluorodeoxyglucose positron emission tomography/computed tomography predicts malignancy grade and prognosis of operable breast cancer: a multi-institute study. Breast Cancer Res Treat 141(2):269–275. https://doi.org/10.1007/s10549-013-2687-7
16. Aogi K, Kadoya T, Sugawara Y, Kiyoto S, Shigematsu H, Masumoto N, Okada M (2015) Utility of (18)F FDG-PET/CT for predicting prognosis of luminal-type breast cancer. Breast Cancer Res Treat 150(1):209–217. https://doi.org/10.1007/s10549-015-3303-9
17. Akimoto E, Kadoya T, Kajitani K, Emi A, Shigematsu H, Ohara M, Masumoto N et al (2018) Role of (18)F-PET/CT in predicting prognosis of patients with breast cancer after neoadjuvant chemotherapy. Clin Breast Cancer 18(1):45–52. https://doi.org/10.1016/j.clbc.2017.09.006
18. Rousseau C, Devillers A, Sagan C, Ferrer L, Bridji B, Campion L, Ricaud M et al (2006) Monitoring of early response to neoadjuvant chemotherapy in stage II and III breast cancer by [^{18}F] fluorodeoxyglucose positron emission tomography. J Clin Oncol 24(34):5366–5372. https://doi.org/10.1200/jco.2006.05.7406
19. Sasada S, Masumoto N, Goda N, Kajitani K, Emi A, Kadoya T, Okada M (2018) Dedicated breast PET for detecting residual disease after neoadjuvant chemotherapy in operable breast cancer: a prospective cohort study. Eur J Surg Oncol 44(4):444–448. https://doi.org/10.1016/j.ejso.2018.01.014
20. Fowler AM (2014) A molecular approach to breast imaging. J Nucl Med 55(2):177–180. https://doi.org/10.2967/jnumed.113.126102
21. Garcia Hernandez T, Vicedo Gonzalez A, Ferrer Rebolleda J, Sanchez Jurado R, Rosello Ferrando J, Brualla Gonzalez L, Granero Cabanero D et al (2016) Performance evaluation of a high resolution dedicated breast PET scanner. Med Phys 43(5):2261. https://doi.org/10.1118/1.4945271
22. Nishimatsu K, Nakamoto Y, Miyake KK, Ishimori T, Kanao S, Toi M, Togashi K (2017) Higher breast cancer conspicuity on dbPET compared to WB-PET/CT. Eur J Radiol 90:138–145. https://doi.org/10.1016/j.ejrad.2017.02.046
23. Iima M, Nakamoto Y, Kanao S, Sugie T, Ueno T, Kawada M, Mikami Y et al (2012) Clinical performance of 2 dedicated PET scanners for breast imaging: initial evaluation. J Nucl Med 53(10):1534–1542. https://doi.org/10.2967/jnumed.111.100958

Publisher's Note Springer Nature remains neutral with regard to jurisdictional claims in published maps and institutional affiliations.